## Supplement of

High-resolution GHG inversion system based on WRF-Chem/DART: assimilating continuous in-situ observation to constrain anthropogenic CO<sub>2</sub> and CH<sub>4</sub> emissions in the Korean peninsula

Doyoon Kwon et al.

10 Correspondence to: Jinkyu Hong (jhong@yonsei.ac.kr)

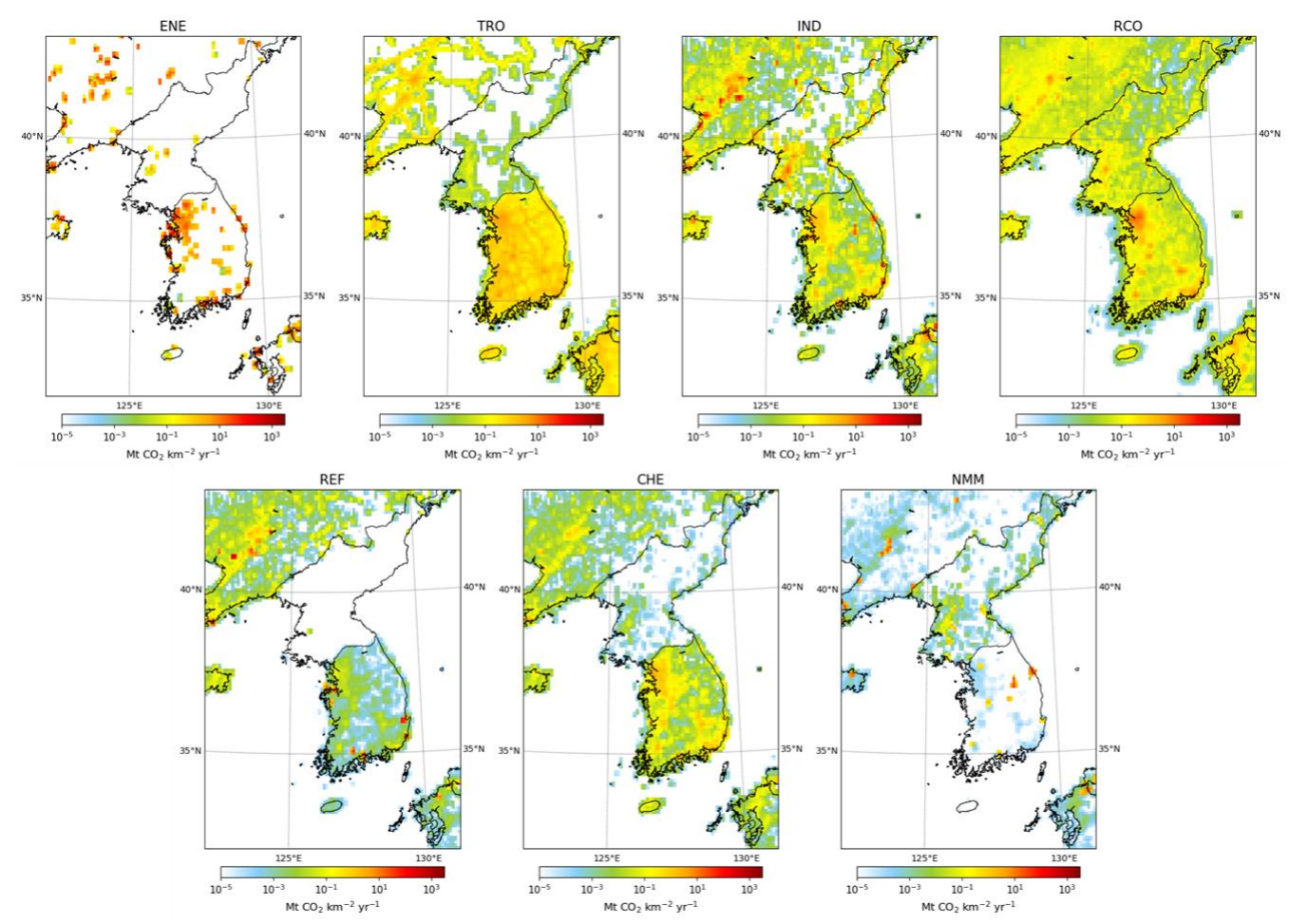


Figure S1. CO<sub>2</sub> emission grid maps by EDGAR sector. Sectors are defined as ENE: power industry, TRO: road transportation, IND: combustion for manufacturing, RCO: energy for buildings, REF: oil refineries, CHE: chemical processes, NMM: non-metallic minerals production

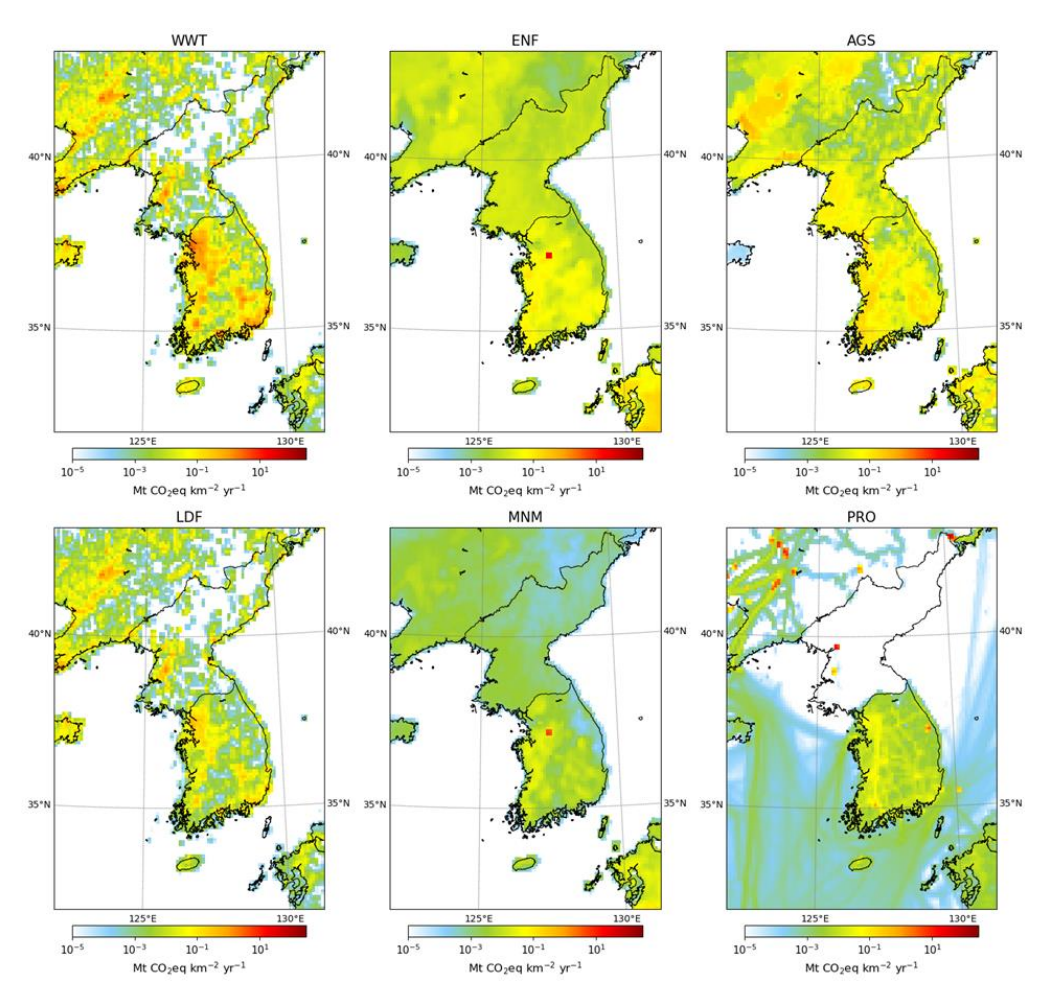


Figure S2. CH<sub>4</sub> emission grid maps by EDGAR sector. Sectors are defined as: WWT: waste water handing, ENF: enteric fermentation, AGS: agricultural soils, LDF: solid waste landfills, MNM: manure management, PRO: fuel exploitation

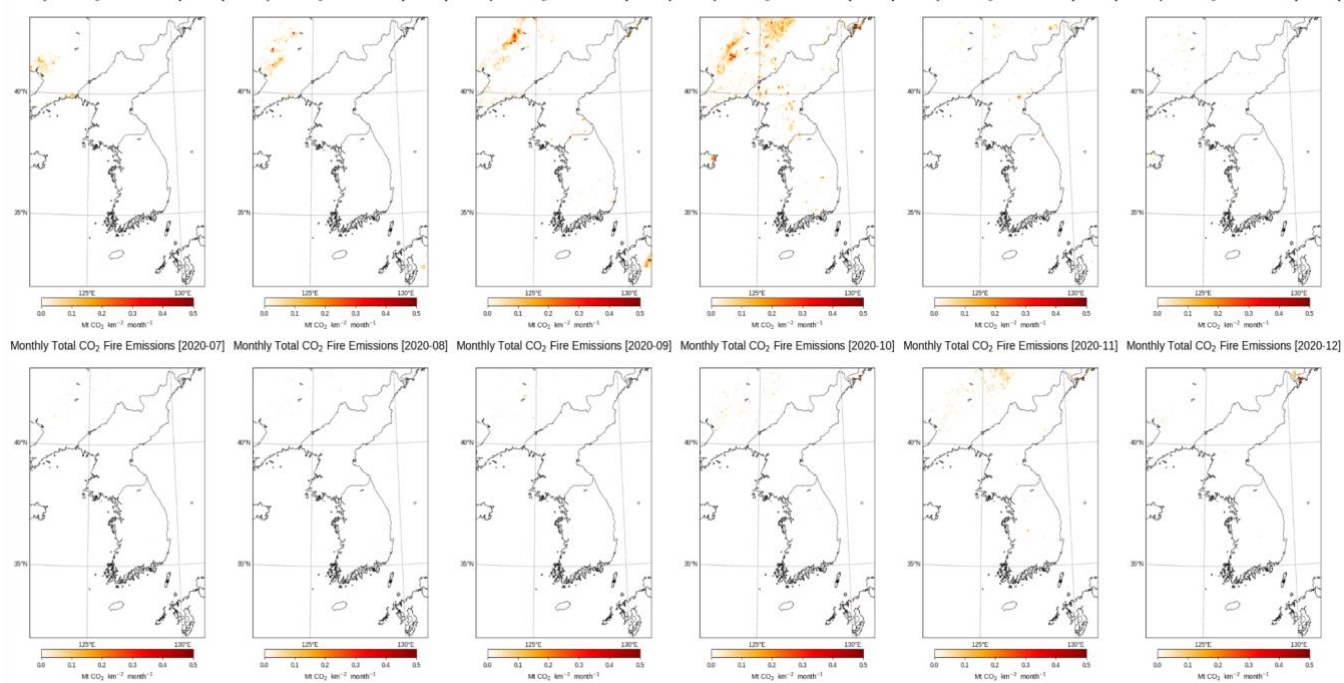


Figure S3. Monthly total CO<sub>2</sub> biomass-burning emissions (Mt CO<sub>2</sub> km<sup>-2</sup> month<sup>-1</sup>) from FINN v2.5 over the model domain in 2020. Strong activity occurs in northeastern China during spring (March–May), with sporadic contributions elsewhere.

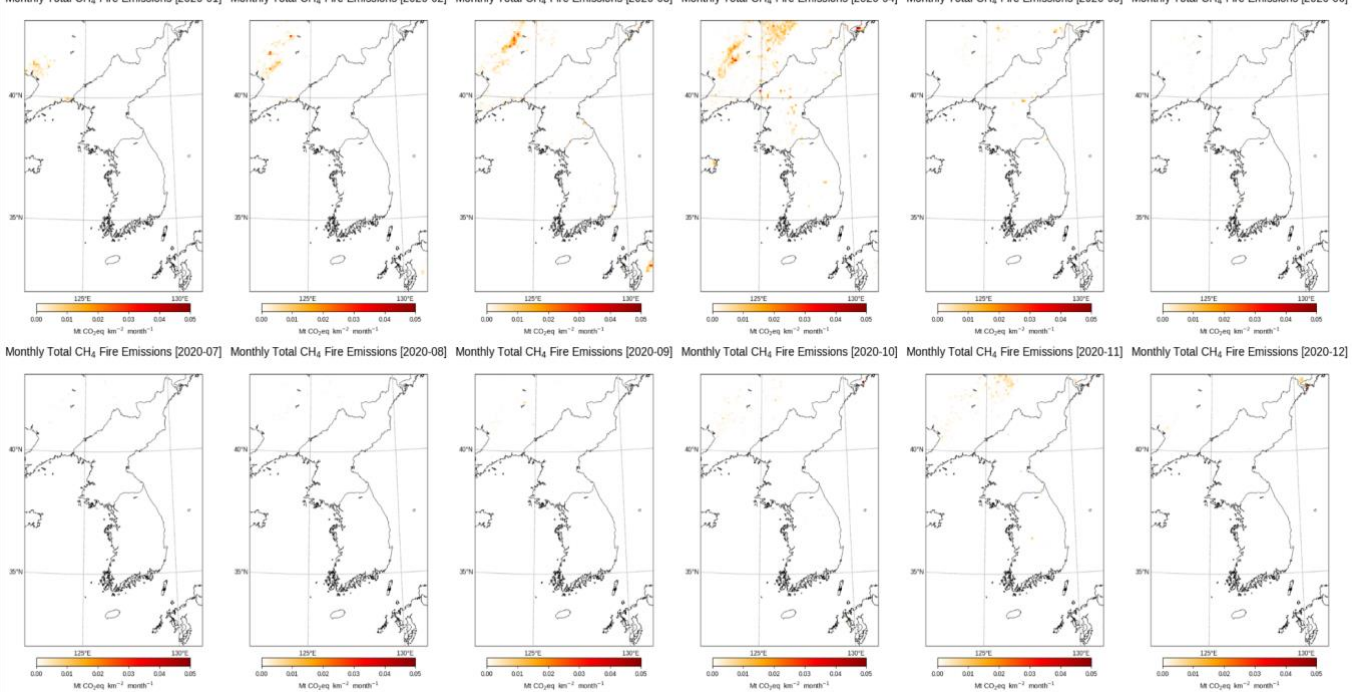


Figure S4. Monthly total CH<sub>4</sub> biomass-burning emissions (Mt CO<sub>2</sub>eq km<sup>-2</sup> month<sup>-1</sup>) from FINN v2.5 over the model domain in 2020, with spatial/seasonal patterns similar to CO<sub>2</sub> but generally lower magnitudes

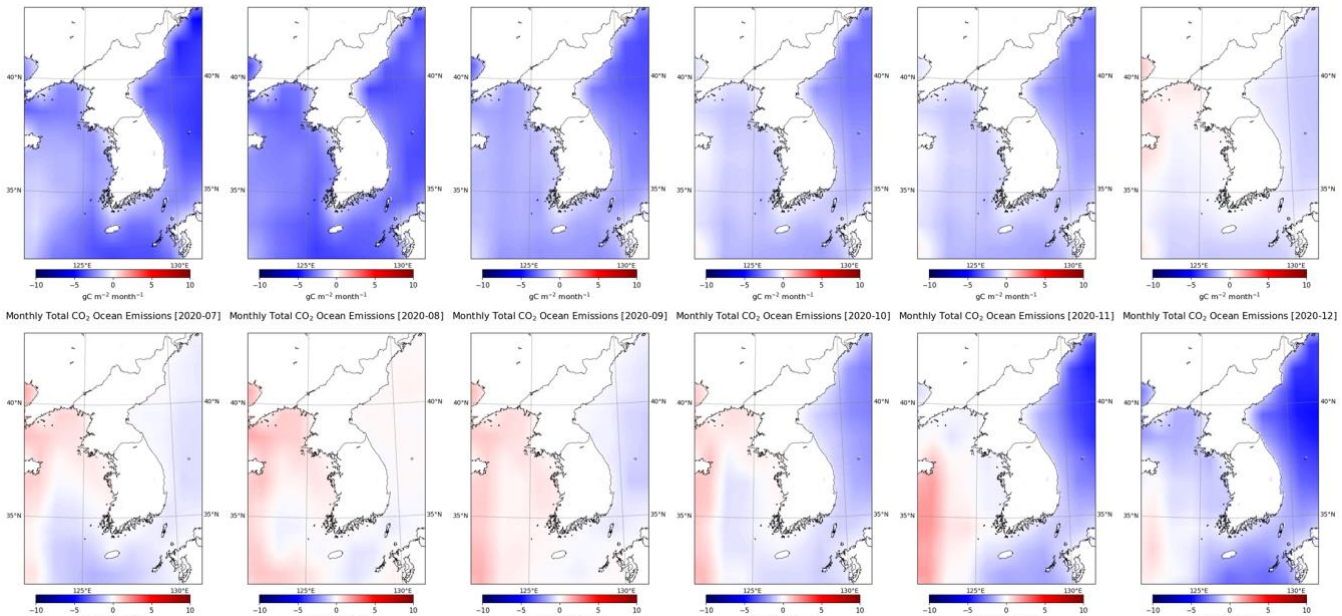


Figure S5. Monthly total ocean-atmosphere CO<sub>2</sub> exchange (gC m<sup>-2</sup> month<sup>-1</sup>) for 2020 from the SeaFlux dataset.

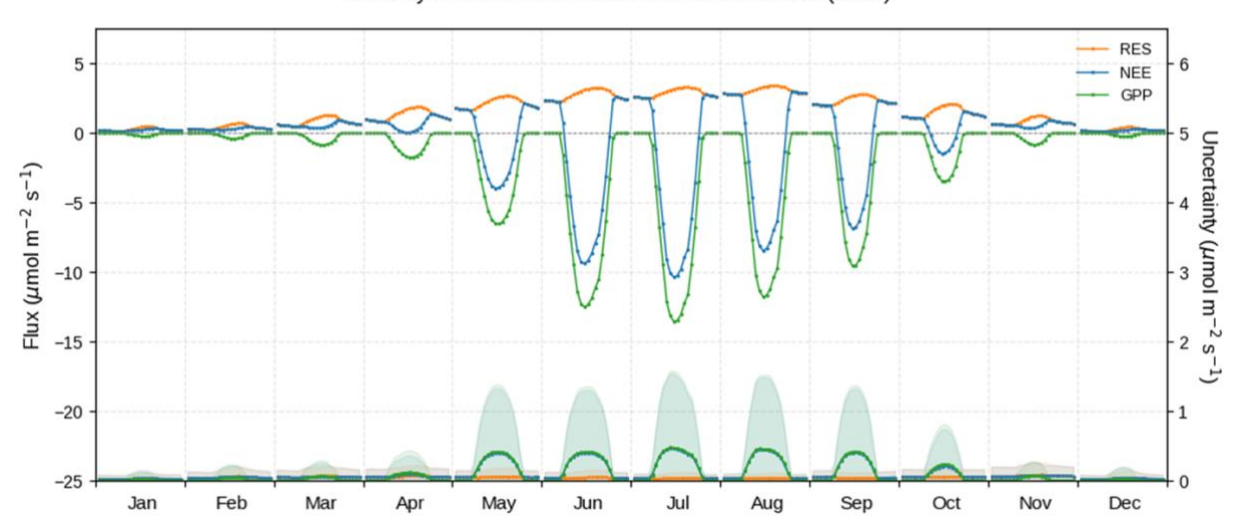
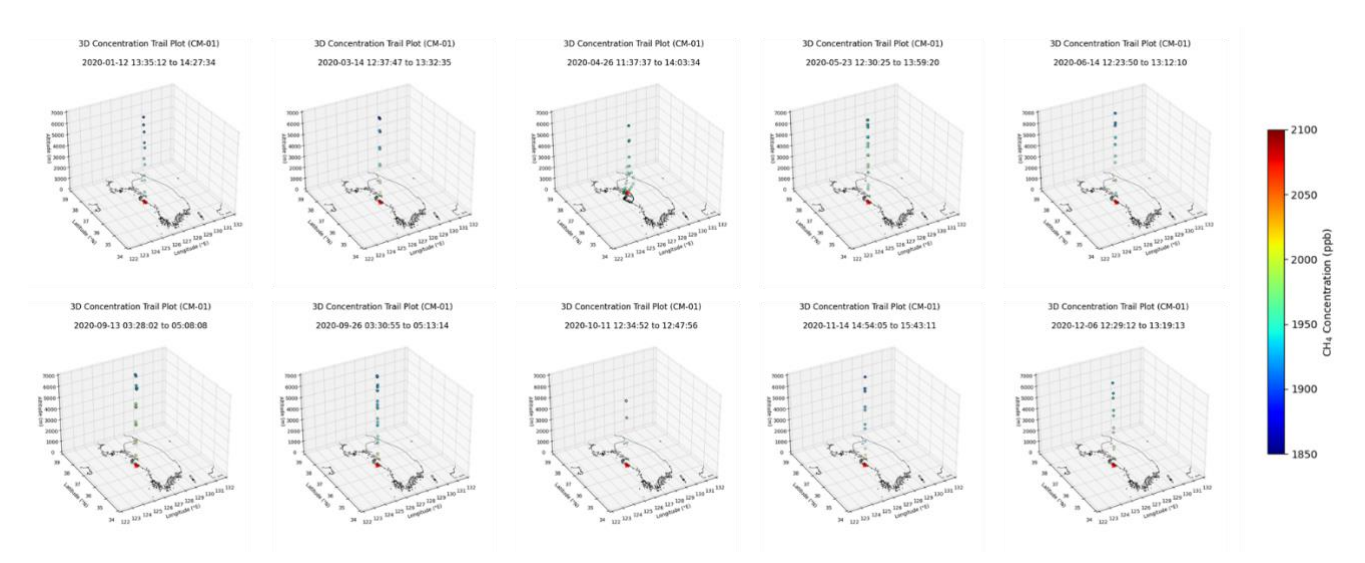


Figure S6. Monthly mean (spatiotemporally averaged) diurnal cycles of gross primary production (GPP), ecosystem respiration (RES), and net ecosystem exchange (NEE) over the model domain in 2020. Solid lines (upper panels) show domain-mean fluxes ( $\mu$ mol m<sup>-2</sup> s<sup>-1</sup>), with shaded bands indicating diurnal standard deviations across grid cells; markers (lower panels) denote corresponding uncertainties, with the secondary y-axis (right) quantifying their magnitude. Peak carbon uptake (negative NEE) occurs in summer due to enhanced GPP, with elevated uncertainties during the growing season.



45 Figure S7. Three-dimensional trajectory plots for the 10 CM-01 vertical-profile flights near AMY in 2020. Panels show flight tracks and corresponding CH<sub>4</sub> concentrations (color scale), sampled at 5-min intervals. These data provide the basis for the mean vertical profiles in Fig. 5 in the main manuscript.

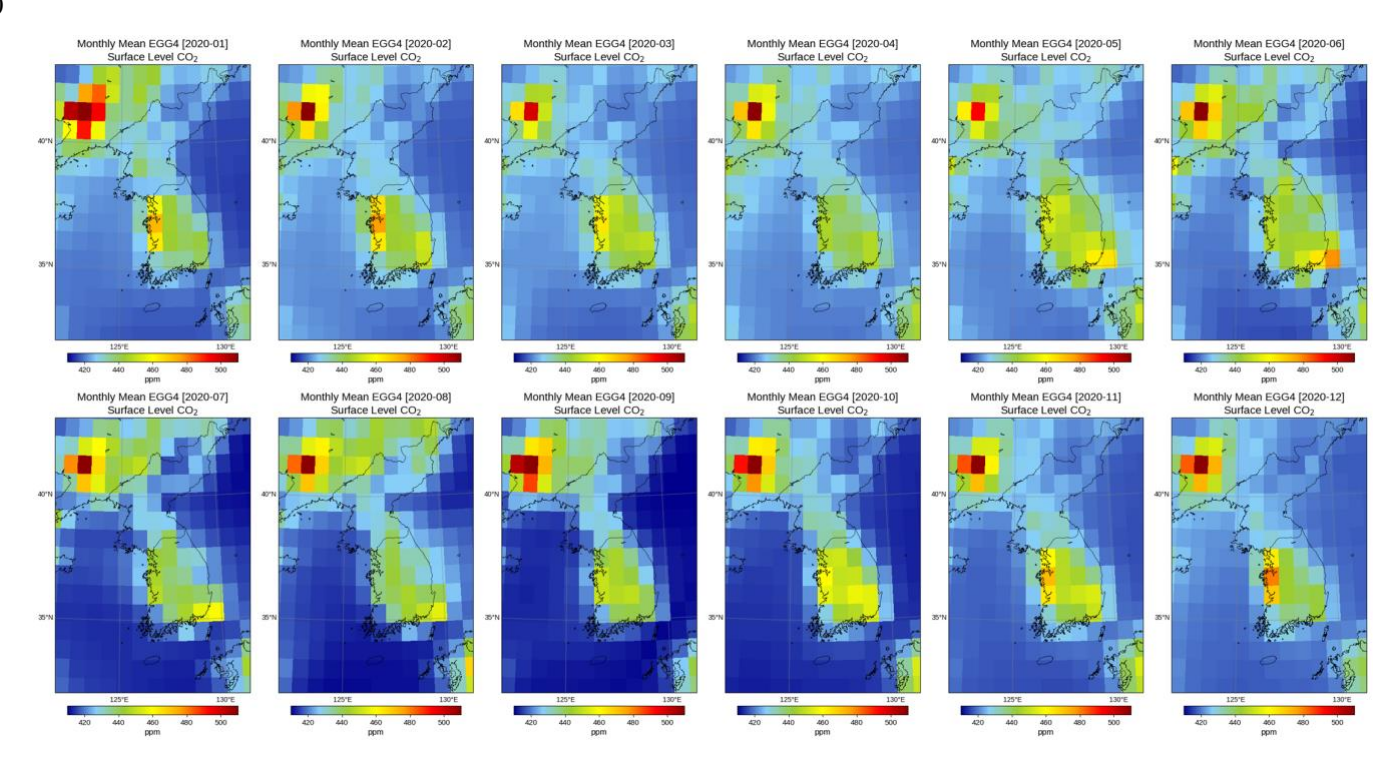


Figure S8. Monthly mean surface CO<sub>2</sub> (ppm) from ECMWF CAMS EGG4 for January–December 2020. These fields are used as initial and lateral boundary conditions in the WRF-Chem/DART inversion. Elevated winter concentrations (e.g., January, February, December) reflect enhanced fossil-fuel emissions and reduced boundary-layer mixing; summer (e.g., July–August) shows lower values due to stronger biospheric uptake and mixing. A uniform color scale facilitates seasonal comparison.

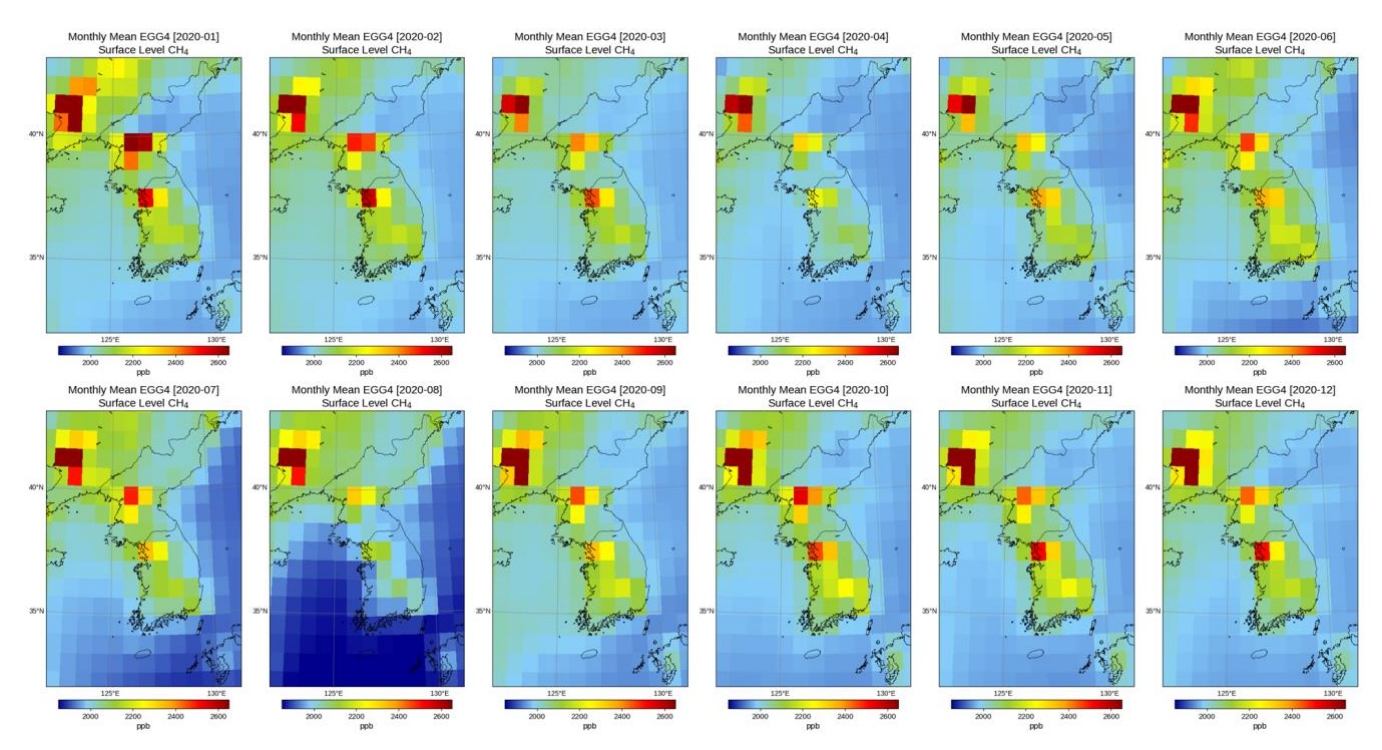


Figure S9. Monthly mean surface CH<sub>4</sub> (ppm) from ECMWF CAMS EGG4 for January–December 2020, used to prescribe initial and lateral boundary conditions. Elevated values persist over northeastern China and the western Korean Peninsula, with a subtle summertime minimum (August) consistent with increased OH-driven loss.

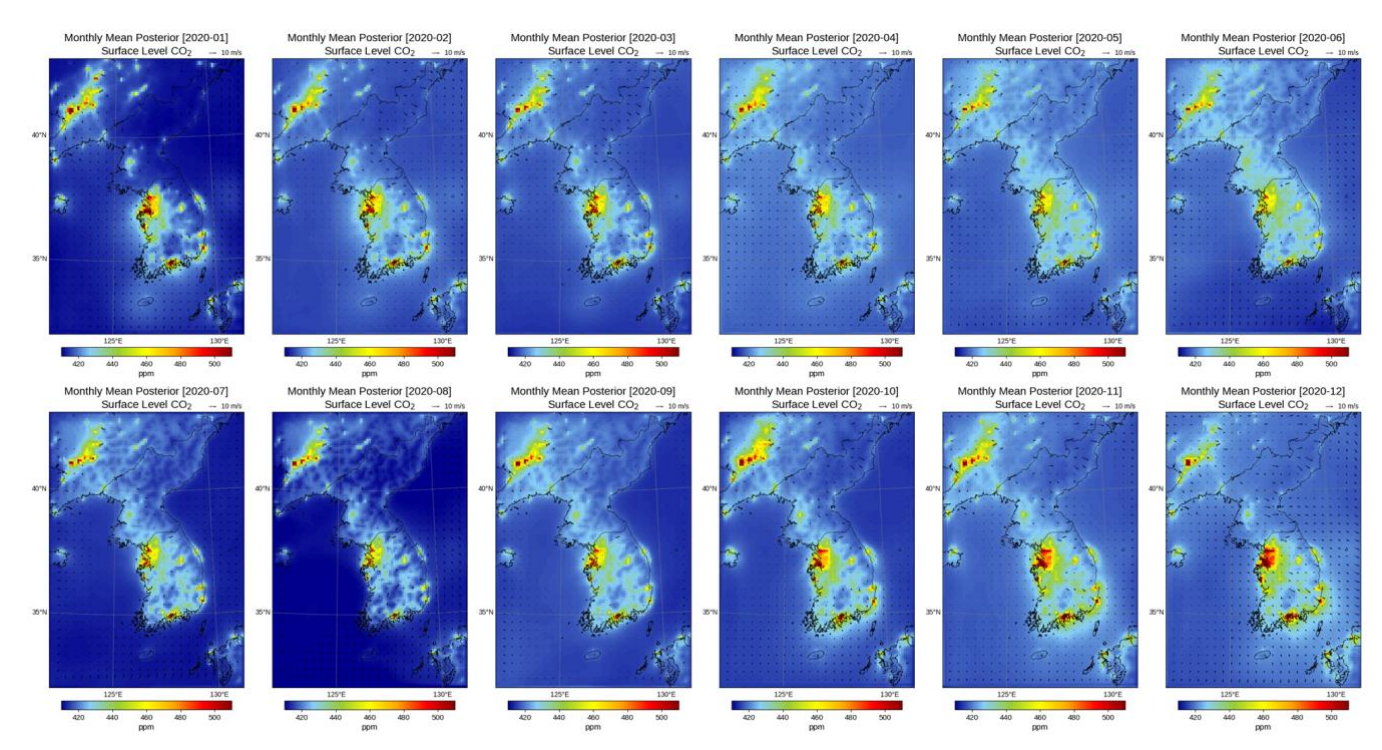


Figure S10. Monthly mean posterior lowest-model-level CO<sub>2</sub> from the WRF-Chem/DART inversion for January-December 2020 over the Korean Peninsula. Maps capture spatial/seasonal variability; enhancements are evident over the SMA, western industrial zones, and southern coastal regions. Summer dilution (July-August) coincides with stronger mixing and biospheric uptake. Wind vectors (10 m) indicate synoptic transport patterns.

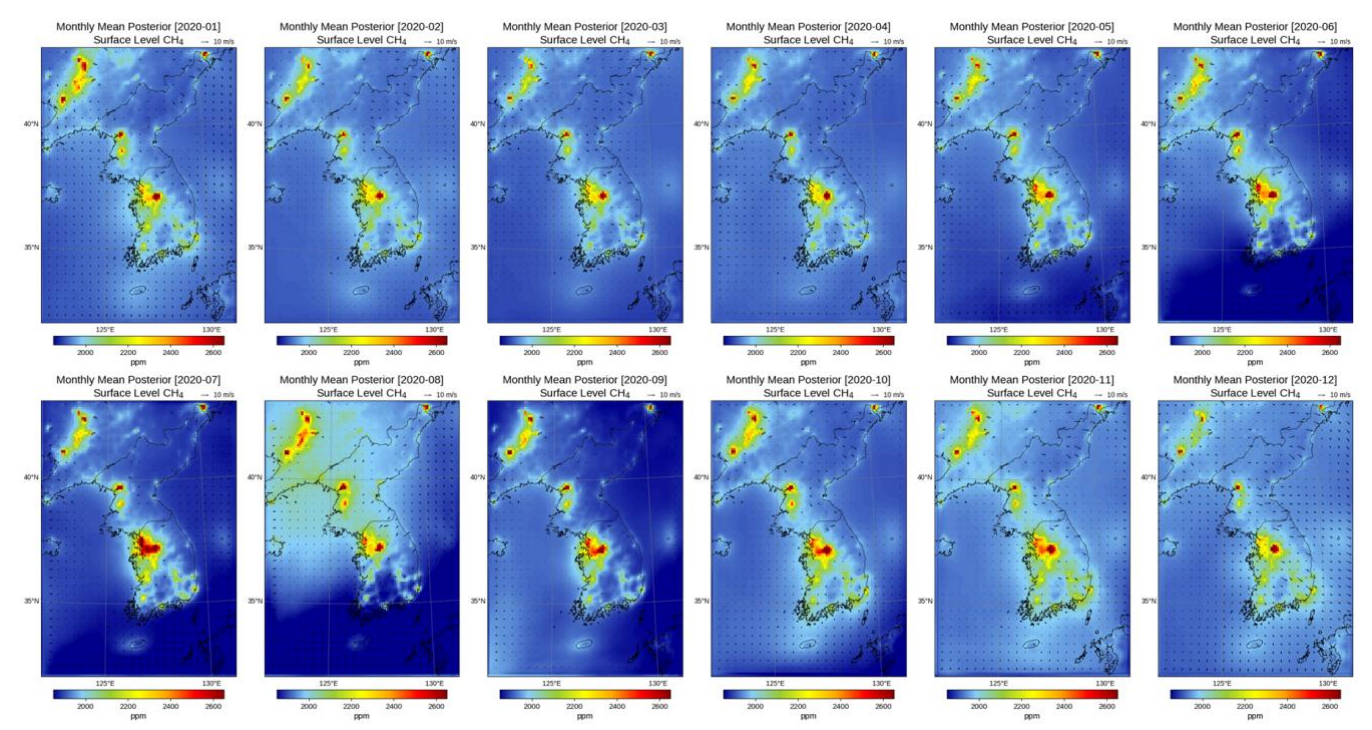


Figure S11. Monthly mean posterior lowest-model-level CH<sub>4</sub> (ppm) for January-December 2020. Enhancements occur over the SMA, central inland regions, and southern coastal zones, with a broad summertime minimum (June-August) consistent with increased oxidation and stronger mixing. Wind vectors (10 m) illustrate prevailing flow.